ISSN: 0067-2904

Laboratory Simulations of Plasma Generated Around the Atmospheric Reentry Spacecraft

Nabaa Ahmed Abdulmuttaleb , Waleed Ibrahim Yaseen*
Department of Astronomy and Space -, College of Science, University of Baghdad, Baghdad-Iraq

Received: 28/9/2023 Accepted: 10/3/2024 Published: 15/11/2024

Abstract

In this paper, plasma will be generated in a laboratory as a simulation of what happens to spacecraft when they enter the atmosphere of Earth. Parameters of plasma generation were determined in terms of pressures of 0.1, 0.2, 0.3, 0.4, and 0.5 mbar and generation energy 200 W. The parameters of the generated plasma were calculated using the optical emission spectroscopy two intensity ratio method, and the electron temperature, electron density, Debye length, and plasma frequency were calculated. Compare the results with the actual results, electron temperatures were 2.26–1.71 eV and plasma frequency 8.09 $x10^{11}$-$6.7x10^{11}$ at 0.1-0.5 mbar pressure.

Keywords: laboratory simulation, plasma generation, optical emission spectroscopy, electron temperature, electron density, pressure, and altitude.

المحاكاة المختبرية للبلازما المتولدة حول المركبة الفضائية العائدة إلى الغلاف الجوي

نبأ احمد عبد المطلب ، وليد ابراهيم ياسين*
قسم الفلك والفضاء، كلية العلوم، جامعة بغداد، بغداد، العراق

الخلاصة

في هذه الورقة ، سيتم إنشاء البلازما في المختبر كمحاكاة لما يحدث للمركبة الفضائية عندما تدخل الغلاف الجوي للأرض. تم تحديد معلمات توليد البلازما من حيث الضغط (0.1، 0.2، 0.3، 0.4، 0.5)ملي بار، وطاقة التوليد 200 واط. تم حساب معاملات البلازما المتولدة باستخدام طريقة التحليل الطيفي للانبعاثات الضوئية ذو الشدة النسبية وتم حساب درجة حرارة الإلكترون وكثافة الإلكترون وطول ديباي وتردد البلازما. وتمت مقارنة النتائج مع النتائج الفعلية. تم الحصول على درجات حرارة الإلكترون(1.17–2.26) فولت وتردد البلازما ($8.09x\ 10^{11}$– $6.7x10^{11}$) هيرتز عند ضغط (0.1–0.5) ملي بار.

1. Introduction

Exploring new planetary frontiers requires dealing with issues related to the design and engineering of heating protection systems to protect a space vehicle from burning re-entry conditions caused by high entry speeds, which are distinguished by extreme heat flux to the spacecraft's nose as well as a sharp increase in the temperature in a shock region. [1], [2].

*Email: waleedib1972cnc@gmail.com

At these load levels, ablation is the only viable approach for thermal protection. A combination of several factors helps heat shields made of ablation materials to withstand high heat loads. The hot surface reduces heat transfer to the wall and increases heat re-radiation; pyrolysis reactions inside the material cause gassing, which at first keeps the hot plasma flow away through the surface; chemical and thermal breakdown uses heat through oxidation, nitridation, and sublimation [3].

The term "plasma" is used to describe a partially or completely ionized gas containing electrons, ions, and neutrals [4] [5].
Ionization of the gas s atoms and molecules occurs simultaneously with the intense heating of the air beyond the shock wave created by the hypersonic flow surrounding the reentry vehicle. During the orbit velocity of entering the Earth's atmosphere (8 km/s), the level of ionization is often less than 0.1%. It is typically possible to ignore how ionization processes affect a vehicle's aerothermodynamic properties, particularly the most delicate variable, and the heat flow to the surface. To pinpoint the electromagnetic wave reflection trajectory segments where a radio communication blackout occurs, the density of electrons in the shock layer must be estimated. When traveling at speeds greater than 10 km/s, ionization processes have a substantial impact chemical makeup and temperature of the shock layer's gas. [6]. The quantity of ions and neutral gas components, as well as the distribution of electron temperature, is the key variables that affect the level of radiation for entrance vehicles. The chemical and physical reactions occur under thermochemical non-equilibriumcircumstances characteristic of the state generated by a shock wave in front of the spacecraft must be taken into consideration. [7]. The flow of gas nears the Stardust capsule, which is the fastest manmade vehicle returning to Earth and has an entrance velocity of more than 12 km/s, was researched by Alex A. and Shevyrin (2018). The effect of plasma parameter distributions on convection and radiation heat fluxes on the vehicle surface has been investigated [8]. In this work can be simulated laboratory of plasma generate around spacecraft during entry from space to the Earth atmosphere using vacuum system also diagnosis plasma parameters and compared with what actually happens in during spacecraft entry in to the Earth atmosphere.

2. Radio Blackout

Because of the ionization of neutral particles that results from the shock wave burning at the spacecraft's nose, a thick plasma layer is produced on the reentry of the spacecraft into the earth's atmosphere. The plasma layer's density measure in spectroscopy technique is reaches 10^{18}–10^{19} m^{-1}, which results in the so-called radio blackout. Radio transmissions generated by the reentry vehicle are unable to connect with ground stations during blackouts because they are deflected by the plasma layer. Understanding reentry plasma properties such as maximum density and density profile is necessary to investigate radio blackouts. Traditionally, electrostatic probes have been used to detect the density of reentry plasma. [9]. Using the reflectometry technique, fusion plasmas are measured. [10], was used to determine the density of the reentry plasma in spacecraft experiments. [11]. The Optical Emission Spectroscopy (OES) technique was used in this study to diagnose plasma parameters.

3. Optical Emission Spectroscopy (OES) technique

The OES method is widely used to identify laboratory plasmas, such as arc plasma, gas discharge plasma, and inductively coupled plasma (ICP) [12] [13]. Numerous analytical approaches have been developed to evaluate plasma properties such as electron density, electron temperature, element identification, and quantification of components present in the plasma. OES was used to analyze various examinations of ICP the plasma systems as a whole, such argon and mixes of many molecular systems, to identify plasma attributes. [14] [15].

3.1 Electron temperature

Because it defines the state of ionization and the population of atoms and ions at different energy levels in terms of plasma temperature and electron density, plasma's ionization model is required to understand spectroscopic data. The approach shown below is applied to obtain the temperature of electrons T_e and electron density n_e for locally thermodynamic equilibrium (LTE) plasmas. [16] [17].

T_e and T_{ext} are connected because free electrons drive the excited state of atoms and molecules. The physical properties of plasma are provided by the emission line intensity. Let's assume that the LTE requirement for the population concentrations of the higher energy levels of both lines is met. In that instance, T_e may be determined simply using the intensity ratio approach. [18]. The electron's temperature was determined by applying the equation to the intensity of each hydrogen emission line in the spectral spectrum (Balmer area). [19] [20]:

$$T_e = \frac{\Delta E}{\ln\left[\frac{A_1 g_1 \lambda_2 I_2}{A_2 g_2 \lambda_1 I_1}\right] K} \quad (1)$$

where E, I, g, K, and A denote the energy difference between the two levels, intensity, wavelength, statistical weighting factor, Boltzmann constant, and transition probability.

3.2 Electron Density

When the plasma is close enough to Local Thermodynamic Equilibrium (LTE) conditions, the number of electrons (n_e) may be calculated by dividing the ratio of the intensity of the two lines corresponding to different ionization phases of a single element (Saha-Boltzmann technique). [21]. The electron density can be calculated as

$$n_e = \frac{\frac{\lambda_1 I_1}{A_1 g_1}}{\frac{\lambda_2 I_2}{A_2 g_2}} 6.04x10^{21} T^{3}/_{2} e^{\left[\frac{(-E_2+E_1-X_1)}{KT}\right]} \quad (2)$$

where I_1 and I_2 are the net emission intensity for the ions and neutrality lines, respectively; statistical weighting product transition probability (g.A) represents the product between the statistical weight and the transition probability, λ nm is the wavelength, n_e is the electron density, X is the ionization energy ; and E_1 and E_2 J are the ion and atom excitation energies, respectively [22].

4. Plasma Parameters

4.1 Debye length

Electrons in plasma are attracted to nearby ions and conceal their electrostatic fields from the remainder of the plasma. In the same way, an electron at rest repels other electrons that are nearby while attracting ions. This effect changes the potential of a charged particle's neighbor. If there is an excess of either negative or positive particles in the plasma, the surplus creates an electric field, and the electrons travel to cancel the charge. The reaction of charged particles to lessen the influence of local electrical fields is known as Debye shielding, and it is this shielding that gives plasma its quasi-neutrality. The electric potential created is predominantly on the particle's surface and extends across a distance λ_D, known by the Debye length, which is defined by [23] [24] [25]:

$$\lambda_D = \sqrt{\frac{\varepsilon_o K T_e}{e^2\, n}} \quad (3)$$

Where ε_o is the permittivity of space, k is the Boltzmann constant, and e is the charge of its constant 1.6 $x10^{-19}$ C [26].

This Second requirement for plasma existence ND >>>1, is determined by the number of particles in the Debye sphere, which depends on the density of electrons and electron temperature. [27]:

$$N_D = \frac{4\pi}{3} n_e \lambda_D^3 \quad (4)$$

4.2 Plasma frequency

The plasma's frequency is a crucial plasma characteristic that distinguishes electron plasma frequencies. This parameter represents the usual frequency of electrostatic oscillations given by the tiny charge separation for electron (e) in a plasma because ofof the small charge separation. Plasma frequency may be computed as [28] [29]:

$$\omega_p = \sqrt{\frac{n_e e^2}{\varepsilon_o m_e}} \quad (5)$$

5. Atmospheric of the Earth

The atmosphere contains a few extremely concentrated gasses, such as oxygen, nitrogen, and argon, in addition to various trace gasses, such as water vapor, methane, carbon dioxide, and ozone. [30]. Because of fluctuations in solar radiation, the atmosphere's temperature, pressure, chemical component particle presence, and electrical properties are all changing. Differences in air characteristics at a specific height were used to convert the altitude variations. Knowing the vertical distribution of parameters such as temperature, pressure, density, and speed of sound is required to pressure altimeter the calibrations, aircraft as well as rocket performance, and the design of their goals, among other things. [31]. Because the real world never remains the same at any time or location, a fictitious model must be created to approximate what may be expected. This model is known as the standard atmosphere. The model considers that the air is devoid of dust, humidity, and water vapor and is at rest with respect to the Earth (no winds or turbulence) [32].

6. Altitude and pressure

The height is determined by the measured barometric pressure. The air density is determined by the barometric pressure and temperature. Gravitation causes air molecules in lower positions to be denser than those in higher positions. It impacts both temperature, and barometric pressure. Because there are fewer molecules in the air at greater elevations, the barometric pressure decreases [33]. Pressure is a commonly managed metric that is strongly tied to industrial production and space applications. Modern detection systems rely heavily on pressure. [34]. The pressure sensor is a BMP 180 barometric pressure, temperature, and altitude sensor. The best low-cost sensing solution for detecting barometric temperature and pressure is the high-precision sensor from Bosch. It can be used as an altimeter because the pressure fluctuates with height. [35].

7. Laboratory Simulations of Plasma

The five-specie model was used in the laboratory simulation. The gas-phase chemical processes in a weakly ionized reentry flow, where the five species that follow may arise in the plasma sheath, are chemical reactions of oxygen, nitrogen, oxygen (O_2, N_2, Ar, and e) [36]. The plasma chamber, vacuum system, and DC high Voltage power source comprise the plasma system. Stainless steel was used to make the anode and cathodes.

7.1 Plasma Chamber

It has a glass chamber with a height, diameter, and thickness of 20 , 30 , and 0.5 cm, respectively. The system's foundation is a stainless-steel flange. Anode and cathodes with the

spacecraft sample confined inside the plasma chamber. It also has an unloading hole and a gas intake hole, as shown in Figure 1.

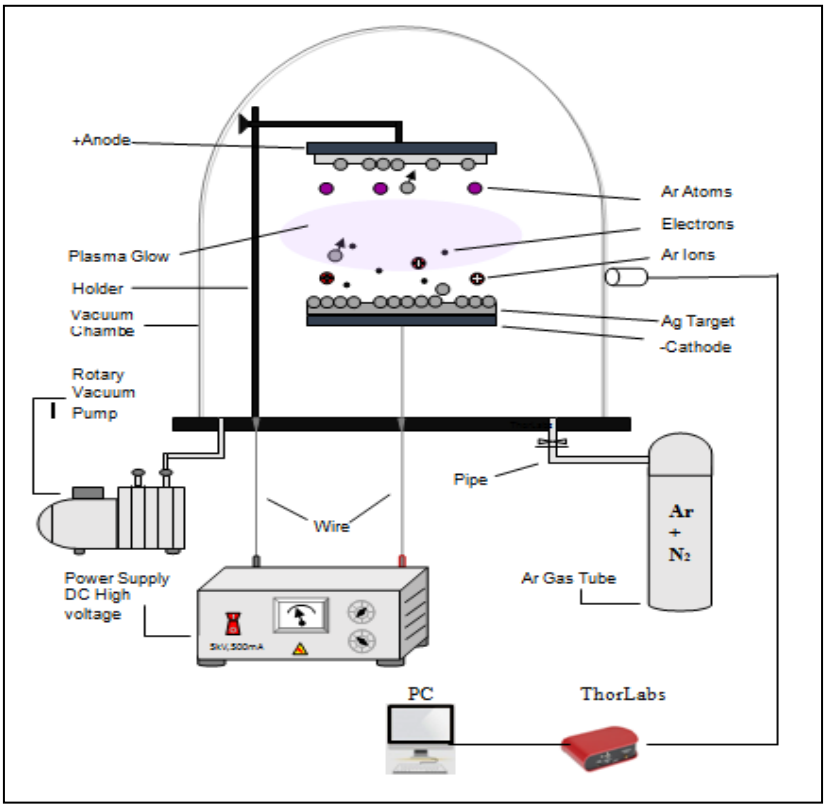

Figure 1: System of laboratory simulations of plasma

The sample a spacecraft was positioned between the anode and the cathode. A two stage rotary pump was used to achieve a vacuum chamber pressure of 0.02 mbar this value represents the maximum value of pressure for the rotary pump. Working gas was argon and N_2, and the operating pressures were 0.1, 0.2, 0.3, 0.4, and 0.5 mbar. From current and voltage power supply the power used was 200 W.. To regulate the gas's pressure inside the chamber, argon and N_2 gas were fed into the chamber via a fine-controlled needle valve (0 – 100) sccm where sccm represents standard cubic centimeter. Thorlabs CCS100/M spectrum spectrometer, optical fiber, and collimating lens were used to obtain the spectrum measurements.

7.2 High Voltage e DC Power Supply

A direct current power supply was employed to produce the plasma. This power produces a voltage of approximately 0–5 kV and a current of 500 mA. The power supply comprises a 5000 V 500 mA transformer, a capacitor, a bridge diode, a voltmeter, and an ammeter.

8. Circuit diagram and code of the barometric pressure device (BPM180 sensor)

A BPM180 sensor was used in this project. The module's name is GY-68. The small device can measure pressure, altitude, and temperature. A simple device that uses BPM180 to determine pressure and altitude Arduino to program for it , and an I2C LCD screen to present that information may be made and placed in the plasma chamber. The scheme of this device is shown in Figure 2.

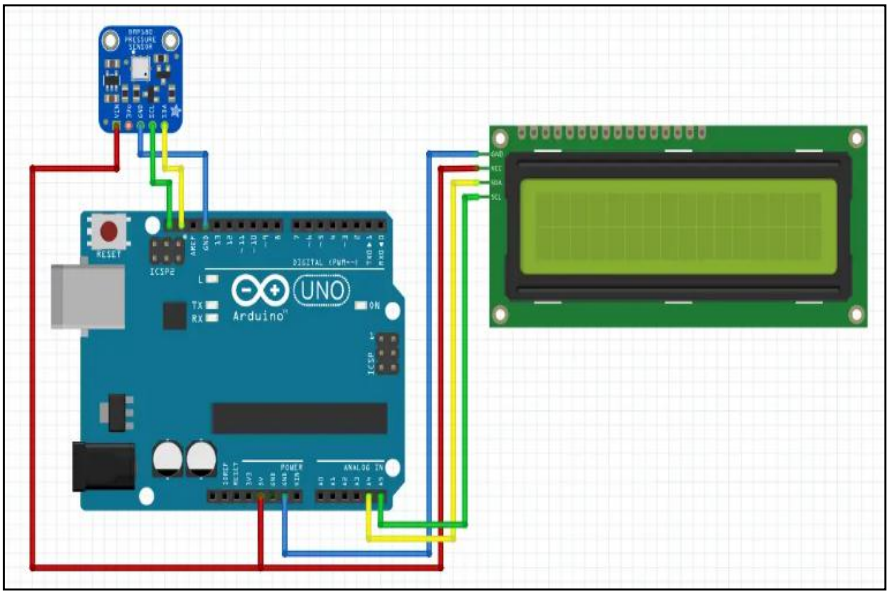

Figure 2: Electronic circuit diagram of **the Arduino barometer** pressure

The following sketch will give you a complete understanding of how to read temperature and barometric pressure from the BMP180 module and can serve as the basis for more practical experiments and projects, The code of the program is shown in Figure 3. This code is important to run barometer pressure.

Every (1 mbar) deviation from sea level pressure leads to approximately (8.5) m of inaccuracy in height estimations. Therefore, the altitude we are obtaining is close but not exact. If this sea level pressure, which varies with weather, is known, an accurate height measurement may be obtained. The current pressure at sea level is assumed to be 1013.25 mbar in this code. A pressure gage was installed within the plasma system to track the pressure and height during operation.

```
#include <Wire.h>
#include <Adafruit_BMP085.h>
#define seaLevelPressure_hPa 1013.25
Adafruit_BMP085 bmp;
void setup() {
Serial.begin(9600);if (!bmp.begin()) {
Serial.println("Could not find a valid BMP085 sensor, check wiring!");
while (1) {}}}
void loop() {
    Serial.print("Temperature = ");
    Serial.print(bmp.readTemperature());
    Serial.println(" *C");
    Serial.print("Pressure = ");
    Serial.print(bmp.readPressure());
    Serial.println(" Pa");
    Serial.print("Altitude = ");
    Serial.print(bmp.readAltitude());
    Serial.println(" meters");
    Serial.print("Pressure at sealevel (calculated) = ");
    Serial.print(bmp.readSealevelPressure());
    Serial.println(" Pa");
    Serial.print("Real altitude = ");}
```

Figure 3: Code of the program BMP180 module

9. Results and Discussion

The emission spectra of the plasma argon and nitrogen produced between the cathode and anode at pressures from 0.1 to0.5 mbar are shown in Figure 4.

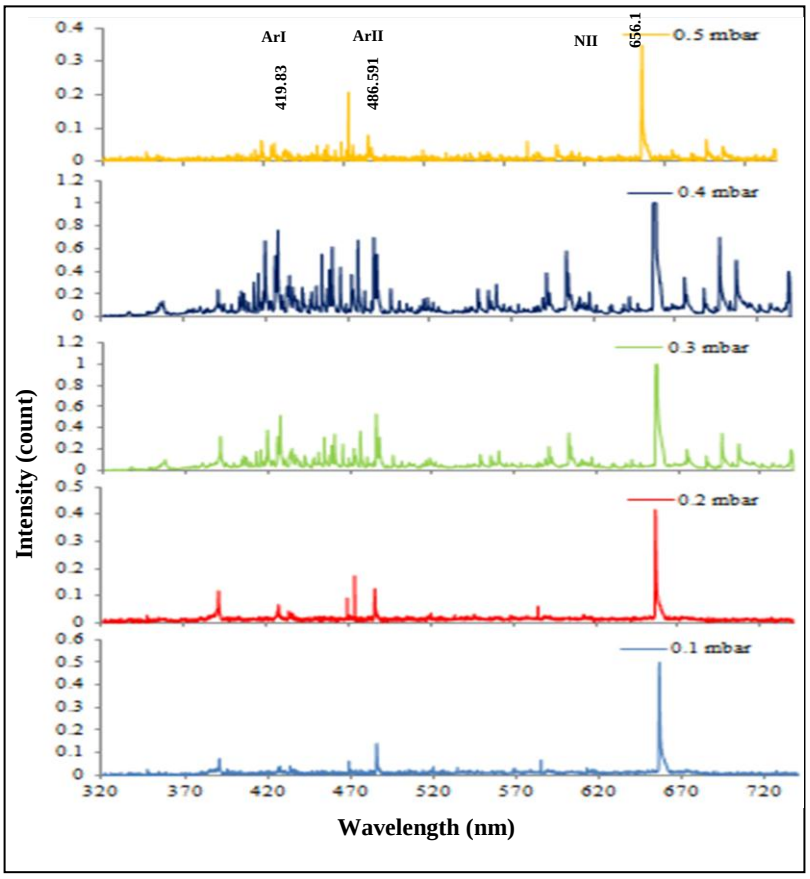

Figure 4: Emission spectra for plasma argon and nitrogen at different pressures.

The strength of the lines rises as the gas pressure increases, with the intensity of the lines being proportional to (p^{β}), where β is a constant that ranges between 0.2 and 0.5 depending on the wavelength. [37] [38]. Figure 5 represents the intensity of the Ar I 419.83 and Ar II 486.591 nm lines as a function of the gas pressure in DC power.

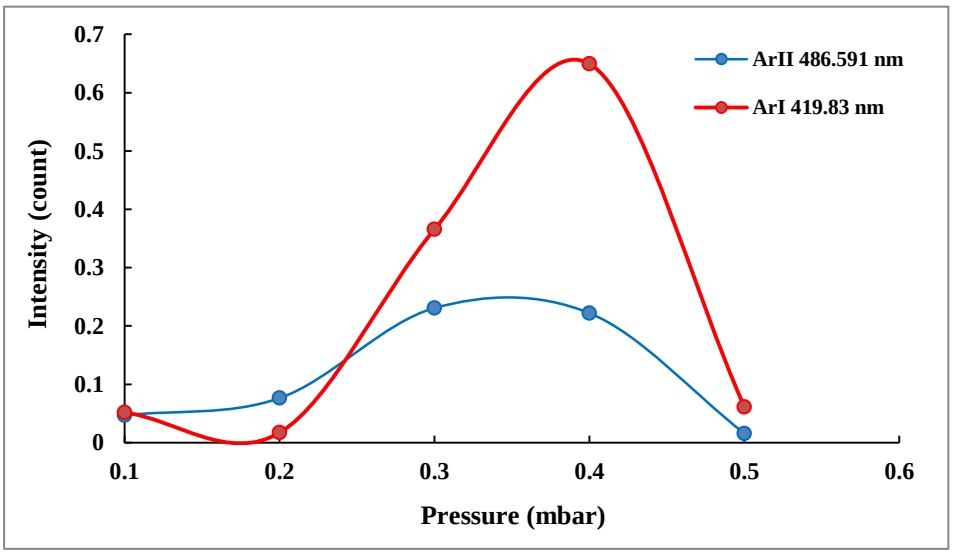

Figure 5: Intensity of Ar I 419.83and ArII 486.591 nm lines.

where the intensity of the ArII 486.591 nm line increases by increasing the gas pressure to a value of 0.649 at 0.4 mbar, and then the intensity decreases to 0.0614 at 0.5 mbar. The intensity of the Ar I 419.83 nm line increases by increasing the gas pressure to a value of 0.222 at 0.4 mbar, and then the intensity decreases to 0.0156 at 0.5 mbar. Two suitable lines, ArI and ArII, are chosen for the estimated electron temperature and electron density using the intensity ratio method. By using NIST, we can obtain line parameters as listed in Table 1.

Table 1: Parameters of Ar I and Ar II lines

λ (nm)	Ag (s^{-1})	E_i (eV)	E_k (eV)
ArI 419.8317	$2.57x10^{+06}$	11.6235	14.5759
ArII 486.591	$9.x10^{+07}$	19.9675	22.5148

The effects of pressure on the electron temperature and electron density of the DC plasma using optical emission spectroscopy are shown in Figure 6. At low pressures, the density of the particles is very low, so the ionization process is weak, i.e., the electron density is low. To compare what happens in the process of returning a spacecraft to the gaseous envelope of the Earth, the energy is low at the beginning of the generation of plasma in the laboratory system, and this is why the electron temperature is low, and after that, the energy increases by increasing the energy of the power supply to 200 W. this occurs when the spacecraft enters the gaseous envelope, which generates friction between the spacecraft and the air, and very high thermal energy is generated, which ionizes the air atoms surrounding the spacecraft, which leads to raising the electron temperature and increasing the electron density. After that, pressure increases as it happens at low altitudes, where the density of air molecules is high, which increases collisions and heat exchange between electrons and air atoms, which reduces the electron temperature. This is exactly what happens in the return process, as the speed of the spacecraft decreases at low altitudes, which reduces the friction process with particles. Thus, the energy that supplies the plasma surrounding the vehicle decreases, the ionization process decreases, the electron density decreases, and the electron temperature decreases, as shown in Figure 6. These results agree with [39].

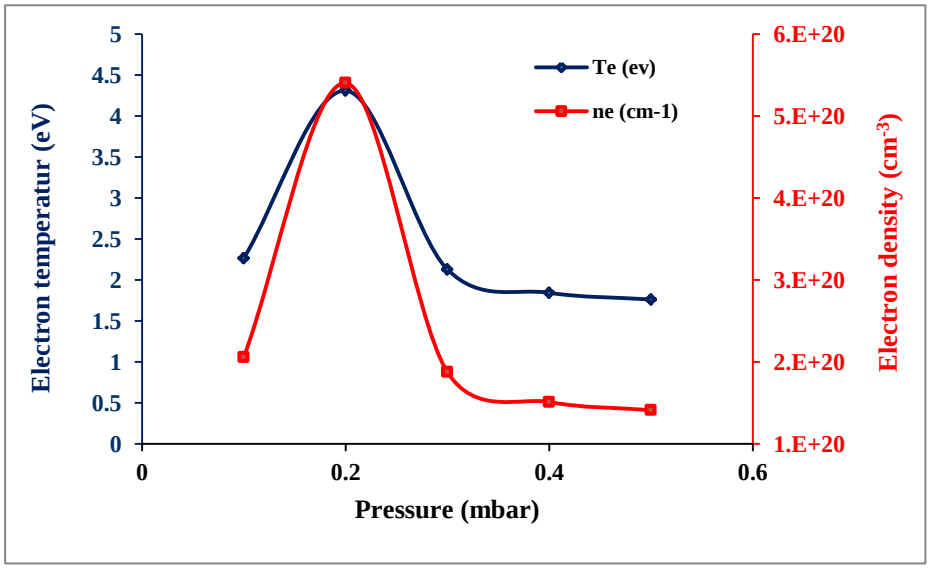

Figure 6: Electron temperature and electron density versus pressure at an input power of 200 W.

Debye length variation with pressure is illustrated in Figure 7. With increase pressure the electron density increase, this will necessitate smaller Debye lengths in order to confrontation the external potential because of their large charge to volume ratio. In low electron density or in low pressure, a larger layer need be formed to accumulate the same amount of electrical charge. The Debye length is also dependent on electron temperature; higher temperatures necessarily involve higher mobility of electrons this results agree with [40]. Figure 7 shows the variation of the plasma frequency with pressure. The plasma frequency increases with electron density according Eq. (5), therefore at increased pressure the number of molecule increase inside the chamber, and thus plasma frequency increase. The laboratory simulations of the plasma parameters are listed in Table 2.

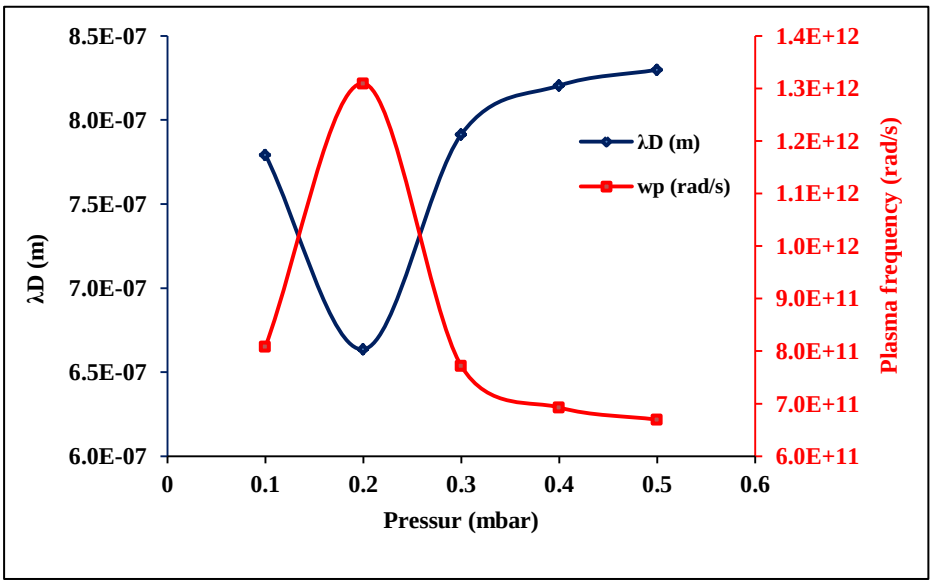

Figure 7: Debye length and plasma frequency versus pressure an input power of 200 W.

Table 2: Laboratory simulations of plasma parameters

Pressure (mbar)	Altitude (km)	Electron temperature (eV)	Electron density (m^{-1}) x10^{20}	λD (m)x10^{-7}	Plasma frequency (rad/s)x10^{11}
0.1	65	2.26	2.06	7.79	8.09
0.2	60	4.30	5.40	6.64	13.1
0.3	57	2.12	1.88	7.91	7.72
0.4	55	1.84	1.51	8.20	6.93
0.5	53	1.76	1.41	8.30	6.7

Conclusions

It has been shown that the strength of the lines of emission spectra of laboratory-generated argon plasma is highly dependent on external variables such as gas pressure. After generating plasma in the laboratory and conducting a diagnosis of the plasma parameters, it was noted that the electron temperature decreases with increasing pressure, while the electronic density increases with increasing pressure due to the increase in the number of molecules. This is what actually happens when the spacecraft enters the gaseous atmosphere. The pressure increases when the height of the spacecraft decreases. The comparison used in this work with laboratory simulations of the spacecraft reentry process was nearly consistent. This practical study can be used to study the plasma generated around spacecraft entering the Earth's atmosphere.

References

[1] C. Roberto, I. Armenise, M. Cacciatore, M. Capitelli, F. Esposito, P. Gamallo and a. R. K. Janev, "Atomic and molecular data for spacecraft re-entry plasmas," *Plasma Sources Science and Technology,* vol. 25, no. 3, p. 033004, 2016.

[2] J. L. Stollery, "Hypersonic and High-Temperature Gas Dynamics," *The Aeronautical Journal* , vol. 111, no. 1116, p. 121, 2007.

[3] J. C. O., P. A. Gnoffo and a. A. Mazaheri, "Influence of coupled radiation and ablation on the aerothermodynamic environment of planetary entry vehicles.," no. NF1676L-16461, 2013.

[4] I. K. Abbas, M. U. Hussein, M. H. Hasan and a. H. H. Murbat, "The Effect of the Non-Thermal Plasma Needle on Pseudomonas Aeruginosa Bacteria," *Iraqi Journal of Science,* vol. 58, no. 3A, pp. 1214-1219, 2017 .

[5] T. A.Hameed and a. H. R.Humud, "Comparison Study of Plasma-Activated Water and Plasma Jet Effects on Escherichia coli Bacteria for the Disinfection of Tooth Root Canal," *Iraqi Journal of Science,* vol. 64, no. 12, pp. 6285-6293, 2023.

[6] C. O. Johnston, Nonequilibrium shock-layer radiative heating for Earth and Titan entry, Virginia Tech, 2006.

[7] S. G. V., Y. A. Bondar, G. P. Oblapenko and a. E. V. Kustova, "Development and testing of a numerical simulation method for thermally nonequilibrium dissociating flows in ANSYS Fluent," *Thermophysics and Aeromechanics,* vol. 23, no. 2, pp. 151-163., 2016.

[8] S. A. A., T. Y. Shkredov, G. V. Shoev and a. Y. A. Bondar, "Modeling of the plasma environment of re-entry space vehicles," in *AIP Conference Proceedings*, 2018.

[9] L. J. J. W. and a. A. E. Cross, "Electrostatic probe measurements of plasma surrounding three 25000 foot per second reentry flight experiments," *NASA Special Publication,* vol. 252, p. 109, 1971.

[10] S. F., "Measurement of electron density profile by microwave reflectometry on tokamaks," *Review of scientific instruments,* vol. 56, no. 5, pp. 664-669, 1985.

[11] W. Deng, L. He and a. X. Shiyao, "The microwave reflectometers at reentry spacecraft and plasma sheath diagnosing results analysis," *IEEE*, pp. 17-20, 1990.

[12] H. R. Humud and a. S. Hussein, "Optical emission spectroscopy for studying the exploding copper wire plasma parameters in distilled water," *Iraqi Journal of Physics* , vol. 15, no. 35, pp. 142-147, 2017 .

[13] N. K. Hussein and a. S. J. Kadhem, "Spectroscopic Diagnosis of Arc Carbon and Magnesium Plasma," *Iraqi Journal of Science,* vol. 63, no. 6, pp. 2492-2501, 2022.

[14] L. Hood-Hong, "Analytical methods in plasma diagnostic by optical emission spectroscopy: A tutorial review.," *Journal of Science and Technology* , vol. 6, no. 1, 2014.

[15] Y. W. Ibrahim, A. F. Ahmed, D. A. Al-Shakarchi and a. F. A.-H. Mutlak, "Development of a high-power LC circuit for generating arc plasma and diagnostic via optical emission spectroscopy," *Applied Physics A*, vol. 128, no. 2, p. 148, 2022.

[16] H. I. P., "Optical diagnostics for thin film processing," *Elsevier*, 1992.

[17] A. S. Wasfi, H. R. Humud and a. M. E. Ismael, "Spectroscopic measurements of the electron temperature in low pressure microwave 2.45 GHz argon plasma," *Iraqi Journal of Physics,* vol. 13, no. 27, pp. 14-23, 2015.

[18] D. D. M., L. V. Rodriguez-Restrepo and a. a. E. R. Parra, "Methods employed in optical emission spectroscopy analysis: a review," *Ingeniería y ciencia,* vol. 11, no. 21, pp. 239-267, 2015.

[19] A. M. Waqar, M. S. Rahman, S. Choi, U. Shaislamov, J.-K. Yang, R. Suresh and a. a. H.-J. Leea, "Measurement of electron temperature and number density and their effects on reactive species formation in a dc underwater capillary discharge," *Applied Science and Convergence Technology,* vol. 26, no. 5, pp. 118-128, 2017 .

[20] A. K. A., "Spectroscopic study for plasma parameters in co-sputtering system," *Iraqi Journal of Physics* , vol. 14, no. 31, pp. 122-128, 2016.

[21] K. A. Aadim, "Characterization of Laser induced cadmium plasma in air," *Iraqi Journal of*

Science , vol. 56, no. 38, pp. 2292-2296, 2015.

[22] L. Drogoff, B. J. Margot, M. Chaker, M. Sabsabi, O. Barthelemy, T. W. Johnston, F. V. S. Laville and a. a. Y. V. Kaenel, "Temporal characterization of femtosecond laser pulses induced plasma for spectrochemical analysis of aluminum alloys," *Spectrochimica acta part B: Atomic spectroscopy* , vol. 56, no. 6, pp. 987-1002, 2001.

[23] A. I. K. and a. K. A. Aadim, "Spectroscopic Diagnosis of Cobalt Plasma Produced by OES Technique and Influence of Applied Voltage on Plasma Parameters," *Abbas, Ibrahim K., and Kadhim A. Aadim. "Spectroscopic Diagnosis of Cobalt Plasma Produced by OES Technique and Influ Iraqi Journal of Science*, pp. 2271-2281, 2023.

[24] S. N. Mazhir, N. A. Abdullah, H. I. al-Ahmed, N. H. Harb and a. N. K. Abdalameer, "The effect of gas flow on plasma parameters induced by microwave," *Baghdad Science Journal*, vol. 15, no. 2, pp. 0205-020, 2018.

[25] A. S. Wasfi, H. R. Humud, A. H. Muhammad and a. M. S. Al-Ansari, "Characterization of Argon Plasma Induced by Simple 2.45 GHz Microwave Source," *International Review of Physics* , vol. 7, no. 1, pp. 64-69, 2013.

[26] N. F. Majeed, M. R. Naeemah, A. H. Ali and a. S. N. Mazhir, "Spectroscopic analysis of clove plasma parameters using optical emission spectroscopy," *Iraqi Journal of Science*, vol. 62, no. 8, pp. 2565-2570, 2021.

[27] H. R. K., M. A. Aswad and a. R. K. Hassan, "Study the plasma parameters due to the different energies for laser produced lead oxide plasma," *Indian J. Nat. Sci*, vol. 10, no. 57, pp. 17908-17914, 2019.

[28] H. R. H. and a. a. S. Hussein, "Optical emission spectroscopy for studying the exploding copper wire plasma parameters in distilled water," *Iraqi Journal of Physics*, vol. 15, no. 35, pp. 142-147, 2017.

[29] T. A. Hameed and a. S. J. .Kadhem, "Plasma diagnostic of gliding arc discharge at atmospheric pressure," *Iraqi Journal of Science*, vol. 60, no. 12, pp. 2649-2655, 2019.

[30] H. H. Omran and a. W. I. Yaseen, "Estimation of the Standard Atmospheric Earth Model Parameters at 86 km Altitude," *Iraqi Journal of Science*, pp. 4570-4578, 2023.

[31] Y. W. Ibrahim, "Determination of Skip Entry Trajectories for Space Vehicles at Circular and Super Circular Speeds," *Iraqi Journal of Physics* , vol. 8, no. 12, pp. 29-34, 2010.

[32] M. Z. Jacobson, Fundamentals of atmospheric modeling, Cambridge university press, 1999, pp. 2601-2613.

[33] S. J. Endro and a. A. Setyawan, "Altitude Measurement in Topographic Mapping Based on Barometric Pressure, Temperature, and Humidity using Neural Network." International Journal of Scientific Research and Management (IJSRM) 11, no. 05 (2023): 17," *IJSRM*, vol. 11, no. 5, p. 17, 2023.

[34] S. Shayama and a. L. Abraham, "Intelligent pressure measuring system," *International Journal of Computer Schiente and Mobile Computing* , vol. 3, p. 129, 2014.

[35] A. Taqi, F. M. E. Dean and a. K. Rehman, "Senior Design Project Report," 2021.

[36] C. Shao, D. Tian, K. Qian and a. W. Chen, "Numerical simulation of weakly ionized dynamic plasma for reentry vehicles," *Journal of spacecraft and rockets* , vol. 53, no. 5, pp. 900-911, 2016.

[37] A. K. A., S. N. Mazhir, N. K. Abdalameer and a. A. H. Ali, "Influence of gas flow rate on plasma parameters produced by a plasma jet and its spectroscopic diagnosis using the OES technique."," *In IOP Conference Series: Materials Science and Engineering*, vol. 987, no. 1, p. 012020, 2020.

[38] F. U. Khan, N. U. Rehman, S. Naseer, M. A. Naveed, A. Qayyum, N. A. D. Khattak and a. M. Zakaullah, "Diagnostic of 13 . 56 MHz RF sustained Ar – N2 plasma by optical," *Eur. Phys. J. Appl. Phys.*, vol. 45, no. 11002, 2009.

[39] T. C. H. Kang and a. M. K. Bae, " Optical Emission Diagnostics with Electric Probe Measurements of Inductively Coupled Ar/O2/Ar-O2 Plasmas," *J. Physics of Plasmas*, vol. 19, pp. 5-7, 2012.

[40] B. Shokri, M. Abbasi and a. S. Hosseini, "FTIR Analysis of Silicon Dioxide Thin Film Depositedby Metal Organic-Based PECVD," *J. ISPC, Bochum, Germany,* vol. 19, no. 3, 2009.